The EMBO Journal vol.9 no.13 pp.4347-4358, 1990

The *CHL1(CTF1)* gene product of *Saccharomyces cerevisiae* is important for chromosome transmission and normal cell cycle progression in G_2/M

Sandra L.Gerring, Forrest Spencer and Philip Hieter

Department of Molecular Biology and Genetics, The Johns Hopkins University Medical School, 725 N. Wolfe Street, Baltimore, MD 21205, USA

Communicated by D.Nathans

We have analyzed the *CTF1* gene, identified in a screen for mutants with decreased chromosome transmission fidelity and shown to correspond to the previously identified *chl1* mutation. *chl1* null mutants exhibited a 200-fold increase in the rate of chromosome III missegregation per cell division, and near wild-type rates of marker homozygosis on this chromosome by mitotic recombination. Analysis of the segregation of a marker chromosome indicated that sister chromatid loss (1:0 segregation) and sister chromatid non-disjunction (2:0 segregation) contributed equally to chromosome missegregation. A genomic clone of *CHL1* was isolated and used to map its physical position on chromosome XVI. Nucleotide sequence analysis of *CHL1* revealed a 2.6 kb open reading frame with a 99 kd predicted protein sequence that contained two PEST sequences and was 23% identical to the coding region of a nucleotide excision repair gene, *RAD3*. Domains of homology between these two predicted protein sequences included a helix-turn-helix motif and an ATP binding site containing a helicase consensus. Mutants lacking the *CHL1* gene product are viable and display two striking, and perhaps interrelated, phenotypes: extreme chromosome instability and a delay in cell cycle progression in G_2/M. This delay is independent of the cell cycle checkpoint that requires the function of the *RAD9* gene.

Key words: cell cycle/*CTF1* gene/mutants/*Saccharomyces cerevisiae*

Introduction

Accurate chromosome transmission is necessary for cellular viability and the prevention of aneuploidy. Functional domains within the chromosomal DNA (determinants in *cis*) as well as the coordinated activity of many proteins (determinants *in trans*) during the cell cycle are required for chromosome transmission. Cytological studies in a variety of organisms have provided a detailed description of chromosome dynamics within the mitotic cell cycle, but an understanding of the mechanisms underlying chromosome transmission will require biochemical and genetic approaches as well.

Saccharomyces cerevisiae is an excellent organism in which to undertake a genetic analysis of *cis* and *trans* determinants of chromosome segregation. Mutations that perturb chromosome transmission will often cause the loss or gain of chromosomes. Since yeast cells are relatively tolerant of whole chromosomal aneuploidy, mutant strains can grow despite relatively high levels of chromosome missegregation compared with wild-type. The ability to monitor changes in chromosome number facilitates the development of assays for detecting and analyzing mutants defective in chromosome transmission. As a result, a number of genes important for chromosome transmission have been identified and are currently under study in *S.cerevisiae* (reviewed in Newlon, 1988). We have recently described a genetic screen that makes use of an artificial chromosome and a visual ploidy assay to identify mutants defective in *c*hromosome *t*ransmission *f*idelity (*ctf* mutants, Spencer *et al.*, 1990). We anticipated that *ctf* mutations would identify proteins in expected as well as unknown components of the molecular machinery for replication and segregation.

Since the chromosome cycle must be coordinated with the cell cycle, the *ctf* mutations were also predicted to identify genes affecting regulatory systems that monitor the completion of certain events before allowing the cell cycle to proceed. There is evidence for such 'checkpoint' controls in the cell cycle of *S.cerevisiae* (Reed, 1980; Weinert and Hartwell, 1988; Hartwell and Weinert, 1989; Russel *et al.*, 1989). Such control points may be observed as a cell cycle progression delay; for example, the G_2/M delay mediated by *RAD9* in response to DNA damage (Weinert and Hartwell, 1988). Control points may also be revealed as a cell cycle terminal arrest; for example, the *cdc* mutants most clearly involved in DNA metabolism are *RAD9* dependent for their cell cycle arrest phenotype (Weinert and Hartwell, 1988; Hartwell and Weinert, 1989). The *RAD9* gene product appears to be part of a cell cycle checkpoint control that responds to DNA metabolic defects. Since a deletion of the *RAD9* gene causes a 21-fold increase in the rate of chromosome loss (Hartwell and Weinert, 1989), we might expect to identify this gene, and others like it, in the *ctf* collection.

We present a detailed study of a gene, *CTF1 (CHL1)*, identified among a set of mutants isolated solely on the basis of their effects on chromosome stability. Selection of mutants by this primary criterion may allow the description of previously undescribed mechanisms essential for chromosome transmission fidelity. *CTF1* is the largest *ctf* complementation group, consisting of 30 of 136 *ctf* mutants isolated. Here we show that *CTF1* is identical to a previously identified chromosome loss gene, *CHL1*. Haber and colleagues showed that strains carrying the *chl1-1* allele exhibit a dramatic increase in the frequency of chromosome missegregation with a less pronounced effect on the frequency of mitotic and meiotic recombination (Haber, 1974; Liras *et al.*, 1978). They also showed that the frequency of recovery of diploid cells carrying a monosomy is higher for some chromosomes than others (Liras *et al.*, 1978). In this paper, we present an analysis of the chromosomal loss phenotype caused by mutations in *CHL1*

(CTF1) as well as the cloning, determination of the physical map position, and sequence analysis of the gene. In addition, we show that *chl1* null mutants exhibit a G_2/M delay that is independent of *RAD9* function, suggesting that failure to execute *CHL1* function leads to a checkpoint controlled cell cycle delay in or closely preceding mitosis.

Results

CTF1 (CHL1) is important for the fidelity of chromosome transmission

We wished to measure the effect of *ctf1* mutations on chromosome transmission. Genetic markers can be lost either by missegregation of the chromosome that carries them (i.e. generation of a cell with a nucleus lacking a whole chromosome), or as a result of mitotic recombination between homologous chromosomes. Hartwell and Smith (1985) have shown that *cdc* mutants that are defective in DNA metabolism increase both chromosome missegregation and mitotic recombination under semipermissive growth conditions. They further suggested that the *cdc* mutations that increased chromosome missegregation without increasing mitotic recombination might lie in genes involved in chromosome segregation rather than DNA metabolism. To determine the relative rates of these two events in a *ctf1/ctf1* null mutant, we monitored the mitotic segregation of two markers, *MATa* and *LEU2*, located on opposite arms of chromosome III (Figure 1). Homozygosis of *MATα* by mitotic recombination, as well as chromosome III missegregation, will allow these diploids to mate with a *MATa leu2* mating tester to form a triploid. Missegregation of chromosome III can be distinguished from homozygosis of *MATα*, since the former leads to Leu^-3n-1 triploids (*leu2/leu2/−*) and the latter to Leu^+3n triploids (*leu2/leu2/LEU2*) (Figure 1). The results are presented in Table I. *ctf1-Δ1/ctf1-Δ1* diploids missegregate chromosome III at a rate of 3.14×10^{-3}, 200-fold higher than wild-type controls. In contrast, *ctf1Δ1/ctf1Δ1* diploids become homozygous at the *MATα* locus by mitotic recombination at a rate of 8.6×10^{-6}, which is only 3-fold higher than wild-type. Thus, the absence of *CTF1* dramatically increases chromosome III missegregation rates above wild-type levels and has little effect on mitotic recombination. By this criterion, there is no evidence for a role for *CTF1* (*CHL1*) in DNA metabolism.

ctf1 (chl1) mutants exhibit both loss and gain of a chromosome fragment

To understand further the chromosome transmission defect of *ctf1* mutants, we examined the relative contribution of the two types of missegregation events, chromosome loss (1:0 segregation) and chromosome non-disjunction (2:0 segregation). Three heteroallelic *ctf1/ctf1 ade2-101/ade2-101* diploid strains (see Materials and methods), each containing a *SUP11*-marked chromosome fragment, were plated on solid media. *ade2-101* leads to the accumulation of a red pigment that can be suppressed by *SUP11* in a dosage dependent manner. Diploid *ade2-101/ade2-101* cells containing one copy of a *SUP11*-marked chromosome fragment are pink. Cells containing two copies of the *SUP11* marked chromosome fragment are white (Hieter *et al.*, 1985). Thus, colonies derived from cells in which a 1:0 missegregation event occurred in the first division are pink/red half-sectored; similarly colonies derived from cells in which a 2:0 missegregation event occured will be white/red half-sectored. Of colonies founded by cells containing a single chromosome fragment, the percentage that are half-sectored is a measure of the sum of chromosome fragment loss plus non-disjunction. The color phenotype of the half sectors revealed that *ctf1/ctf1* heteroallelic diploids

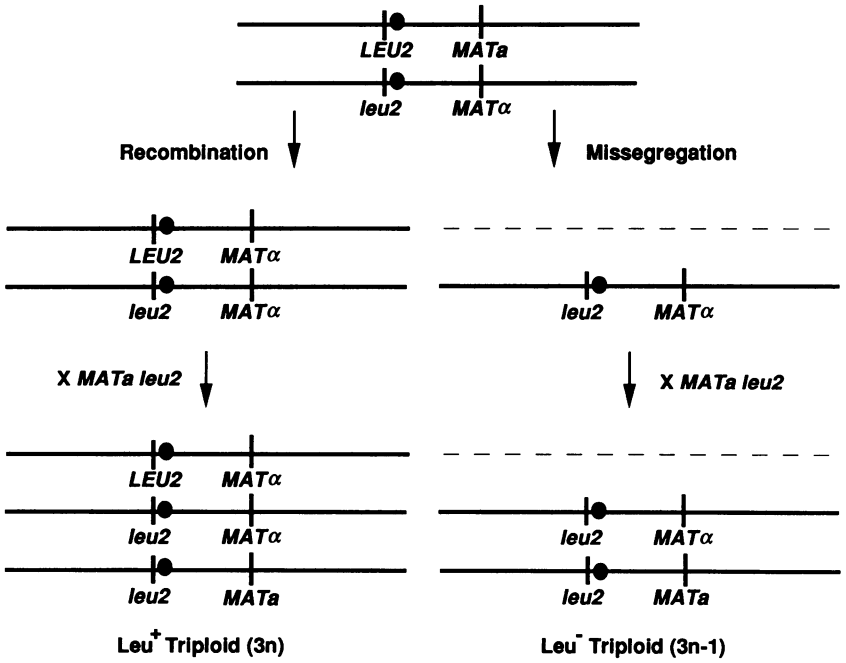

Fig. 1. Determination of chromosome missegregation and marker homozygosis rates in *ctf1-Δ1/ctf1-Δ1.CTF1/CTF1* and *ctf1-Δ1/cft1-Δ1* diploids are *MATaLEU2/MATαleu2*. Missegregation of chromosome III bearing *MATa* will allow mating with a *MATa leu2* mating tester to form Leu^- 3n−1 triploids. Homozygosis by mitotic recombination between *CEN3* and *MAT* will allow mating with a *MATa leu2* mating tester, but the triploid will be Leu^+ 3n.

exhibited an approximately equal distribution between 1:0 and 2:0 events at rates at least 100-fold above wild-type (Table II). Thus, it is clear that both chromosome loss and chromosome gain are occurring in *ctf1 (chl1)* mutant diploids.

Cloning of CTF1 (CHL1)

Plasmids containing the *CTF1* gene were identified by visual screening for complementation of the sectoring phenotype of *ctf1 leu2* mutants. Two strains (YCTF112 and YCTF113) were each independently transformed with plasmid DNA containing a yeast genomic library of 10−12 kb fragments inserted into a *CEN/LEU2* based vector. Leu^+ transformants giving rise to homogeneously white (non-sectored) colonies were candidates for yeast cells containing a genomic clone of *CTF1* (Figure 2). A subset of these candidates was identified which showed a clear coreversion to *ctf1 leu2* by plasmid loss. The requirement for coreversion excluded *ctf1* revertants from subsequent analysis, as well as false positives due to accumulation of the chromosome fragment by non-disjunction prior to transformation, and double transformants containing plasmids in addition to *ctf1* complementing clones. Plasmid DNA was recovered in *Escherichia coli* from two independent transformants of YCTF112 and from one transformant of YCTF113. Restriction fragment analysis indicated that all three plasmids contained overlapping, but not identical, inserts. All three recovered plasmids rescued the *ctf1* sectoring phenotype upon retransformation and therefore contained a *ctf1* complementing genomic segment. The smallest of the three clones, pCTF1-C, contained a 10 kb genomic insert and was selected for subsequent analysis.

The location of the *CTF1* gene was further defined by constructing *Sau*3A partial libraries of this clone and performing Tn*3* transposition mutagenesis (see Materials and methods) on the smallest complementing *Sau*3A clone, pS35 (Figure 3). Constructs obtained during these manipulations were tested for the presence of a functional *CTF1* gene by their ability to complement the sectoring phenotype of *ctf1* mutants. The clones obtained during the various steps in this gene border delineation are depicted in Figure 3 along with their ability or inability to complement a *ctf1* mutant sectoring phenotype. The 3.5 kb insert in pS35R was the smallest complementing clone thus defined. The cloned DNA segment was shown to correspond to *CTF1* by demonstrating genetic linkage between an EMS-induced *ctf1* mutation and a *HIS3* marker integrated at the genomic site of the cloned DNA segment (see Materials and methods).

Chromosomal assignment and physical map position of CTF1(CHL1)

CTF1 was mapped to determine whether it corresponded to a previously identified locus. Assignment to chromosome XVI was achieved by hybridization of a labeled *CTF1* gene fragment to a Southern blot of chromosome-sized DNA (Gerring *et al.*, 1990). To map the physical position of *CTF1* on chromosome XVI, we used a mapping procedure that splits the chromosome at the site of a cloned DNA segment into proximal and distal chromosome fragments (Vollrath *et al.*, 1988; Gerring *et al.*, 1990). Using this procedure to map the *CTF1*-containing DNA, two stably maintained chromosome XVI 'fragments' were generated, and the sizes of these chromosome fragments were determined by analysis of OFAGE gels (Figure 4). This indicated that *CTF1* was 560 kb way from one end of chromosome XVI and 430 kb away from the other end. Assignment of *CTF1* to an arm of chromosome XVI was accomplished by hybridization of a left arm telomere adjacent probe, *GAL4*, to a Southern blot of the OFAGE gel (Figure 4). *GAL4* hybridized to the distal fragment (Figure 4), indicating that *CTF1* was on the left arm of chromosome XVI, 560 kb from the left arm telomere and 430 kb from the right arm telomere.

Allelism of ctf1 to chl1

ctf1 showed tight centromere linkage in meiosis (Spencer *et al.*, 1990) and was physically mapped close to the centromere on the left arm of chromosome XVI, placing *ctf1* close to *chl1* (chromosome loss 1: Haber, 1974). The chromosome missegregation phenotypes of both *ctf1* and *chl1* mutants suggested that they might be allelic. To test for allelism, we constructed the strain YPH576 [*chl1-1 ade2-101 CFVII (RAD2.d.YPH277)URA3 SUP11)*] by standard genetic

Table I. Rates of recombination and chromosome III missegregation in wild-type and *ctf1-Δ1/ctf1-Δ1* mutant diploids

Genotype	*ctf1Δ1/ctf1Δ1*	*CTF1/CTF1*	Ratio
Chromosome missegregation rate	3.14×10^{-3}	1.5×10^{-5}	209
Recombination rate	8.6×10^{-6}	2.7×10^{-6}	3.2

The rates with which mating competent diploids arose by mitotic recombination versus chromosome III missegregation in *CTF1/CTF1* (YPH699) and *ctf1-Δ1/ctf1-Δ1* (YPH700) diploids was analyzed. Mating competent diploids were scored as prototrophic triploids after incubation with a *leu2* mating tester (Figure 1). The fraction of these diploids that had mated due to homozygosis of *MATα* by mitotic recombination were distinguished from those that had missegregated chromosome III, by replica plating to plates lacking leucine. Rates were calculated from these numbers as described in Materials and methods.

Table II. Analysis of chromosome fragment loss and gain frequencies in *ctf1/ctf1* diploids

Gentoype[a]	% 1:0 events[b]	% 2:0 events[c]	Number colonies with 1 CF
ctf1-71/ctf1-157	1.9	2.5	262
ctf1-37/ctf1-112	1.2	3.5	171
ctf1-68/cft1-157	3.8	1.4	212
CTF1/CTF1	0.03	0.03	29 046

Mutants of the above genotypes were plated to single colonies and sectoring phenotypes were scored. Colonies scored as half-sectored were at least 50% red (Koshland and Hieter, 1987). Number of half-sectored colonies scored: YPH770, 9; YPH771, 8; YPH772, 11; YPH279, 20.

[a]Strains used were YPH770, YPH771, YPH772 and YPH279.

[b]Percentage 1:0 events are calculated as number of colonies that are half red:half pink sectored divided by the number of colonies with one chromosome fragment.

[c]Percentage 2:0 events were calculated as above but for half red:half white sectored colonies.

crosses. This strain exhibited a sectoring phenotype at levels comparable with the most severely sectoring *ctf1* mutants. Diploids constructed by mating YPH576 with strains containing various alleles of *ctf1* exhibited chromosome loss by the sectoring assay, indicating a failure of *chl1-1* mutants to complement *ctf1* mutants. In addition, the *chl1-1* sectoring phenotype of YPH576 was complemented by transformation with the cloned *CTF1* gene. We concluded that *ctf1* was allelic to *chl1* and we will henceforth refer to *CTF1* as *CHL1*.

CHL1 is not essential for spore germination or mitotic growth

We used two insertion disruption constructs, In19 and In47 (Figure 3), generated during transposition mutagenesis, to make two independent heterozygous genomic disruptions at *CHL1* by one step gene replacement (yielding YPH715 and YPH716). All four spore products generated from meiosis of either diploid were viable. In addition, all His^+ spores in every tetrad that contained a chromosome fragment exhibited chromosome loss. This indicated that *CHL1* was not essential for spore germination or mitotic growth. Insertions of this type generally disrupt gene function. However, to ensure the absence of *CHL1* function, we constructed a null allele (*chl1Δ1*) in which the amino terminal half of *CHL1* was deleted. Strains containing this allele of *chl1* were also viable. The growth rate and viability of *chl1* null haploids and diploids were not significantly different from wild-type controls (data not shown).

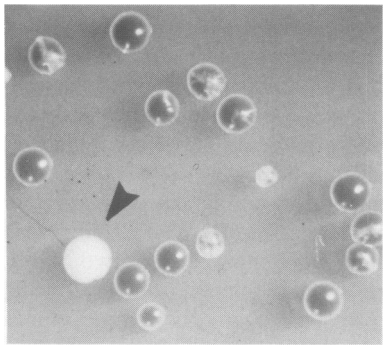

Fig. 2. Identification of *ctf1-112* complementing clones. Candidate transformants containing *ctf1-112* complementing clones were identified by their non-sectoring phenotype. An example is indicated (arrow).

Sequence analysis of CHL1 reveals PEST sequences and homology to RAD3

To ascertain whether there were similarities between *CHL1* and any known proteins or consensus motifs, we sequenced *CHL1*. The nucleotide sequence revealed a 2.6 kb ORF with a predicted protein of 861 amino acids and a molecular weight of 99 kd (Figure 5). PEST sequence analysis (Rogers *et al.*, 1986) identified two PEST sequences in the N-terminal 201 amino acids of the *CHL1* predicted protein (see Figure 5 and Discussion). The *CHL1* predicted protein sequence was also compared with the protein sequences and nucleotide sequence translations of all Genbank libraries. The most significant homology was to the *RAD3* gene (Naumovski *et al.*, 1985; Reynolds *et al.*, 1985), which encodes a 786 amino acid protein known to be involved in nucleotide excision repair (reviewed in Friedberg, 1988). The two proteins were identical in 23%, and similar in 48%, of 422 amino acids with minimal gap allowance. With gap allowance (see Figure 6) the level of identity and similarity remained numerically close, yet extended over 794 amino acids.

Clusterings of amino acid sequence similarity occurred in

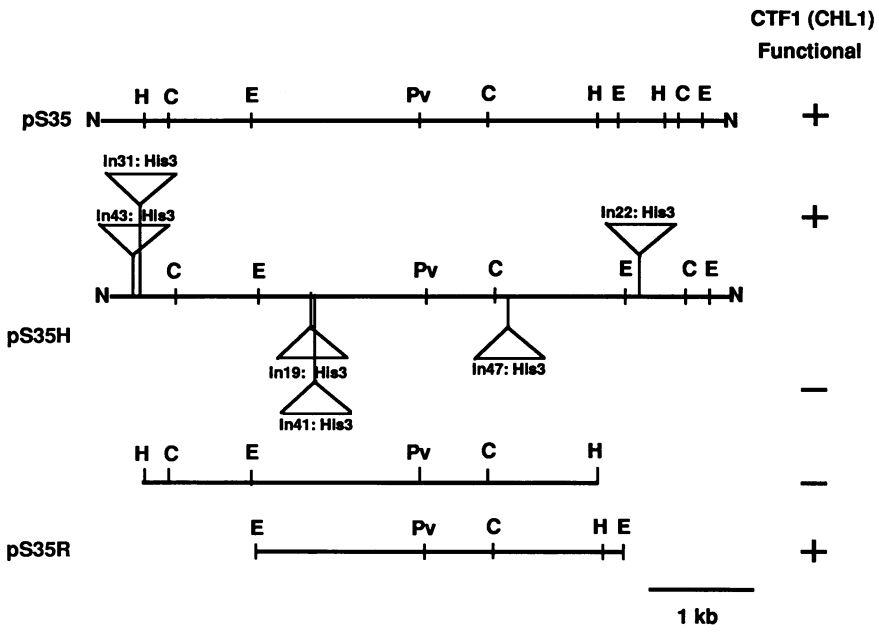

Fig. 3. DNA subclones obtained and tested during border delineation of *CTF1 (CHL1)*. The pS35 insert shown is the smallest *Sau*3− partial fragment of pCTF1-C (original *ctf1* complementing library clone; not shown) that complements *ctf1*. This clone is flanked by *Not*I restriction enzyme sites in the vector pSL40. Tn*3*::*HIS3* insertion mutagenesis (Seifert *et al.*, 1986) of this clone gave rise to the Tn*3* insertions located at the positions marked, and denoted by their In number. Tn*3* insertions drawn below the pS35 insert line disrupted *ctf1* complementing activity. Tn*3*::*HIS3* insertions drawn above the line retained *ctf1* complementing activity. pS35H and pS35R contain *Hin*dIII and *Eco*RI subfragments of the pS35 insert cloned into pRS313. pS35R is the smallest *ctf1* complementing clone depicted. C: *Cla*I, E: *Eco*RI, H: *Hin*dIII, N: *Not*I, Pv: *Pvu*I.

four domains (Figure 6). Domains I and II constitute the A and B motifs of ATP binding proteins (Walker *et al.*, 1982), with the latter showing similarity to the modified B motif suggested for proteins with helicase activity (Linder *et al.*, 1989). Domain IV is in a region of *RAD3* (Naumovski *et al.*, 1985) and a homologous protein, *PIF1* (Foury and Lahaye, 1987), that has been proposed to bind DNA via a helix-turn-helix motif (reviewed in Pabo and Sauer, 1984). To date, no biochemical function associated with the domain III sequence has been demonstrated or hypothesized. Since the homology between the two proteins was significant (see Figure 6 legend), we checked to see whether the *RAD3* gene product could rescue a *chl1* mutant. We were unable to show any qualitative rescue of the sectoring phenotype of eight alleles of *chl1* (data not shown) by *ADH* promoter driven *RAD3* overexpression using pSCW367 (Sung *et al.*, 1987a).

chl1 null alleles exhibit a G_2/M delay in their cell cycle

To determine whether *chl1* mutants exhibited morphological abnormalities compared with wild-type, we examined two independent *chl1* Tn*3* insertion mutants, In19 and In47 (Figure 3). Logarithmically growing cells were fixed with formaldehyde, and stained with a fluorescent dye (DAPI) to visualize the DNA, and with anti-tubulin antibodies (4-124 and 6-345) to visualize the mitotic spindle by indirect immunofluorescence. No abnormal spindle or nuclear morphologies were observed. However, the *chl1* Tn*3* insertion haploids (YPH717 and YPH718), and especially the *chl1/chl1* homoallelic Tn*3* insertion diploids (YPH719) and YPH720), exhibited a significant increase in the number of large budded cells with the nucleus at or in the neck with a short spindle (Table III). Averages of 11% of *chl1* versus 4% of *CHL1* haploid cells, and 32% of *chl1/chl1* versus 5% of *CHL1/CHL1* diploid cells, exhibited this large-budded phenotype (Table III). The bud morphology of these medial nuclear division *chl1* haploid and *chl11/chl1* diploid cells was also abnormal. The bud of the daughter was often as large as that of the mother with the nucleus undivided, a morphology seen very rarely in wild-type cells. Identical results were seen in haploid and diploid *chl1Δ1* null mutants.

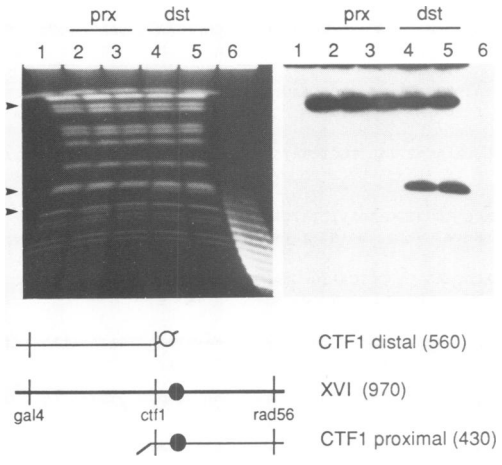

Fig. 4. Mapping the physical position of *CTF1* by chromosome fragmentation. The ethidium bromide stained OFAGE gel on the left shows an electrophoretic karyotype of the parental strain, YPH49 (lane 1). Lanes 2 and 3 show electrophoretic karyotypes of two independent transformants containing the stably inherited *CTF1* chromosome XVI proximal fragment. Lanes 4 and 5 similarly show the electrophoretic karyotype of two independent transformants containing the stably inherited *CTF1* chromosome XVI distal fragment. The gel was blotted to nitrocellulose and probed with *GAL4* (right hand panel). This probe hybridized to the *CTF1* distal fragment and chromosome XVI (top band across all lanes). This indicates that *CTF1* is on the same arm as *GAL4* on chromosome XVI. The sizes (kb) of chromosome XVI and the *ctf1* proximal and distal chromosome XVI fragments are shown.

Since *S.cerevisiae* cells in S, G_2 or early M phases all exhibit a similar microscopic morphology, we analyzed the same populations of cells by flow cytometry to determine the DNA content of these cells. Flow cytometric analysis of haploid and homoallelic diploid strains of *chl1Δ1* (Figure 7) revealed an increase in the proportion of cells with a G_2/M content of DNA. This increase was proportional to the increase in large budded cells observed microscopically. Thus, the data indicates that null and insertion mutant *chl1* haploids and *chl1/chl1* diploids exhibit an accumulation of G_2/M cells.

Despite the accumulation of large budded cells with a G_2/M content of DNA, the growth rate and viability (see Materials and methods) of *chl1* mutants is similar to that of wild-type. This paradox can be resolved by proposing a G_2/M delay and a G_1 (cell separation to bud initiation) acceleration. Cell growth may continue during a G_2/M delay in *chl1* mutants (leading to abnormally large buds) so that at, or even before cytokinesis, the daughter cells have reached the size requirement for start (Reed, 1980). They can therefore proceed immediately into the next cell cycle. This is consistent with the similar cell cycle length of mutants compared to wild-type, the decrease in the number of unbudded cells (Table III), and a 1.4-fold increase in *chl1* mutant cell size at bud initiation (see Materials and methods, data not shown).

The *chl1* G_2/M delay is *RAD9* independent

A *RAD9* mediated G_2/M delay has been documented in wild-type cells in response to DNA damage upon X-irradiation (Weinert and Hartwell, 1988; Schiestl *et al.*, 1989). Since *CHL1* is homologous to a gene that functions in DNA repair, it was possible that in the absence of *CHL1* gene product, lesions were generated or left in DNA that could be recognized by *RAD9*. If this were the case, *RAD9* function would be required for the G_2/M delay phenotype of *chl1* mutants. To test this hypothesis, we made *chl1Δ1 rad9* haploid and homoallelic diploid mutants (YPH743 and YPH750, respectively) and analyzed logarithmically growing cell populations for a G_2/M delay compared with congenic *chl1Δ1 RAD9* strains (YPH744 and YPH747, respectively). As can be seen in Figure 7, the *chl1Δ1 rad9* mutants and *chl1Δ1 RAD9* mutants both exhibited a G_2/M delay not seen in *CHL1 RAD9* or *CHL1 rad9* cells. Therefore the G_2/M delay observed in *chl1Δ1* mutants is *RAD9* independent.

Discussion

The chromosome loss phenotypes of *ctf1 (chl1)* mutants were analyzed in two ways. First, we analyzed whether the *MATa* locus on chromosome III missegregated at an increased rate in *chl1Δ1/chl1Δ1* diploids and whether this occurred by chromosome III missegregation or by mitotic recombination. We found a dramatic increase (200-fold) in the rate per cell division of chromosome III missegregation, and essentially

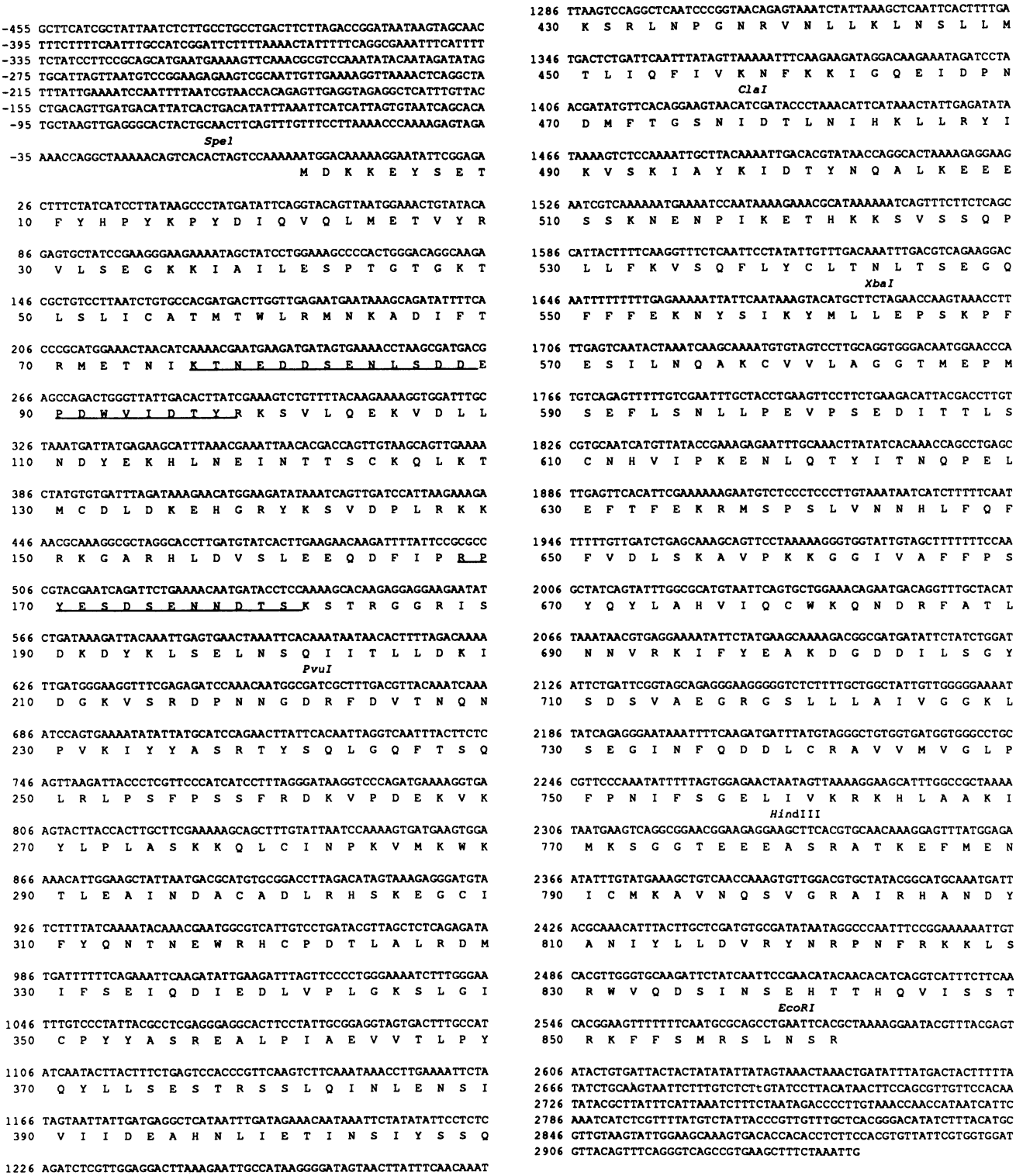

Fig. 5. Nucleotide and predicted protein sequence of *CHL1*. The deduced protein sequence of *CHL1* is assumed to begin with the first methionine of the ORF is shown, and predicts a 99 kd protein. The PEST sequences present in *CHL1* are underlined.

wild-type rates of mitotic recombination. Second, we showed that a chromosome fragment missegregated by both loss and non-disjunction, and that both events occurred at rates 100-fold above wild-type. Although these results do not indicate a particular mechanism for chromosome fragment missegregation (Koshland and Hieter, 1987), the observation of chromosome gain events suggests that missegregation in *chl1* is not due to non-replication of DNA. Taken together, these results suggest that in a *chl1* mutant, sister chromatids are replicated, but missegregate at mitosis by both loss and non-disjunction.

We have shown that *ctf1* is allelic to *chl1* and we will

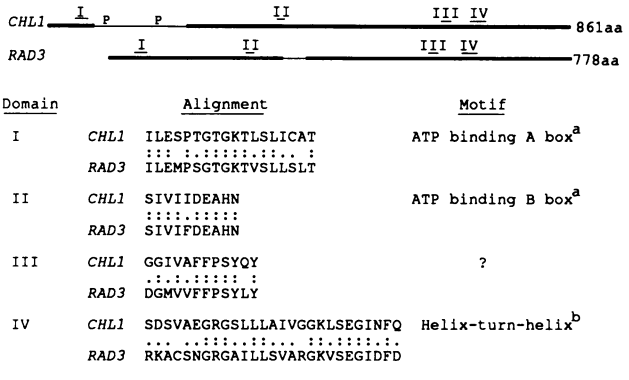

Fig. 6. Domains of amino acid similarity between *CHL1* and *RAD3* predicted proteins. Four domains of similarity were identified. Domains I and II resemble the A and B boxes of the ATP binding domain consensus, with the box B resembling a helicase motif (DEAD box, Linder *et al.*, 1989). Domain IV resembles a helix-turn-helix motif (see Discussion). RDF2 analysis (Dayhoff *et al.*, 1983; Lipman and Pearson, 1985) of the overall similarity between the two proteins (23% identity, 48% similarity) indicated that the homology was significant (init, init0, and opt z value of 26.49, 20.14 and 28.14 s.d. above the mean respectively). Deletion of *CHL1* and *RAD3* sequences in regions demarcated with fine pen lines allows alignment of *CHL1* and *RAD3* over their entire ORF. The location of PEST sequences present in *CHL1* predicted protein are indicated by P's. [a]Walker *et al.* (1982); [b]Naumovski *et al.* (1985); Foury and Lahaye (1987).

Table III. *chl1* mutants show an accumulation of large budded cells with an undivided nucleus[a]

Genotype	*Unbudded*	*Large budded with undivided nucleus*[a]
CHL1	58%	4%
chl1::Tn*19*	54%	12%
chl1::Tn*47*	65%	10%
CHL1/CHL1	59%	5%
chl1::Tn*19*/*chl1*::Tn*19*	39%	30%
chl1::Tn*47*/*chl1*::Tn*47*	37%	35%

Logarithmically growing cells were fixed and processed as for flow cytometry. Bud morphology of >300 cells was determined by phase microscopy for each genotype. The percentage of small budded cells (haploid *CHL1:chl1* = 20%:12%, diploid *CHL1:chl1* = 20%:12%) and large budded cells with separated DNA masses (haploid *CHL1:chl1* = 19%:16%, diploid *CHL1:chl1* = 18%:19%) was similar in all populations.
[a]Large budded, with the bud >0.5 the area of the mother, and with an undivided nucleus at/in the neck.

henceforth refer to *ctf1* as *chl1*. Previous work on the first described allele of this locus (Haber, 1974; Liras *et al.*, 1978) showed that *chl1-1/chl1-1* diploids exhibited monosomy for chromosome III in cell populations at a frequency of ~1%. Furthermore mitotic recombinants were recovered 10-fold more frequently than in wild-type diploids. It was suggested that the loss of chromosomes is non-random, in *chl1-1/chl1-1* mutant diploids (Liras *et al.*, 1978). In *chl1-1/chl1-1* diploids, monosomies for some chromosomes (chromosomes I and III) were recovered at a higher frequency than for other chromosomes (chromosomes II, V, VI, VII, XI and XVII) (Liras *et al.*, 1978). We have not examined this phenotype using alleles isolated in the present study. However, independent isolates of *chl1* missegregate *CEN3*-bearing chromosome III derived fragments as well as *CEN4*-bearing chromosome VII derived

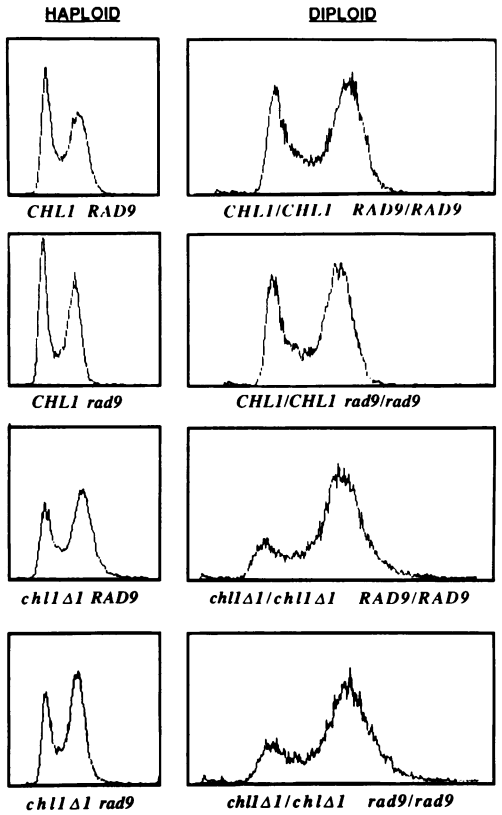

Fig. 7. The accumulated stage in a logarithmically growing population of *chl1Δ1* cells is G_2/M and this accumulation is *RAD9* independent. Cell cycle distribution of the logarithmically growing cultures of the genotypes depicted was analyzed by flow cytometry. The number of cells is depicted on the vertical axis, fluorescent intensity of emitted light (proportional to DNA content) is shown on the horizontal axis.

fragments at similar, highly elevated rates compared with wild-type (Spencer *et al.*, 1990). Possibly, *chl1-1* mutants exhibit a size dependent chromosome loss defect whose analysis is complicated by whole chromosomal aneuploidy associated lethality.

In addition to dramatic chromosome loss, logarithmically growing populations of *chl1* null mutants exhibit a G_2/M delay phenotype. This suggests that lack of *CHL1* function leads to a failure in the execution of a process that normally occurs during G_2/M and that is required for wild-type levels of chromosome stability. In our experience, a G_2/M accumulation does not appear to correlate simply with chromosome loss; only 23% of 62 *ctf* mutants examined (excluding *chl1*) exhibit a clear G_2/M accumulation (unpublished). It is important to point out that flow cytometric analysis does not allow the distinction between late S phase cells and cells on G_2/M. Therefore, despite the lack of evidence for a role for *CHL1* in DNA metabolism, we cannot formally rule out the possibility that the delay occurs in late S phase.

Several hypotheses may be proposed to explain the G_2/M delay in *chl1* mutants. First, *CHL1* could play a direct role in chromosome transmission within G_2/M. In this case, the delay would be imposed by a checkpoint control in G_2/M in response to the recognition of *chl1* associated chromosome transmission defects. Second, it is conceivable that the cell cycle delay is due to a physical barrier to G_2/M progression due to the absence of *CHL1* function. Third, the G_2/M

Table IV. Strains used in this study[a]

S.cerevisiae strain S288C derivatives	Genotype	Source or reference
YPH47	*MATα ura3-52 lys2-801 ade2-101 trp1-Δ1*	
YPH49	*MATa/MATα ura3-52/ura3-52 lys 2-801/lys 801 ade2-101/ade2-101 trp1-Δ1/trp1-Δ1*	
YCTF32[b]	*MATa ura3-52 lys2-801 ade2-101 his3-Δ200 leu2-Δ1 CFIII(CEN3.L.YPH278) URA3 SUP11 chl1-32*	Spencer *et al.*, 1990
YCTF112	*MATa ura3-52 lys2-801 ade2-101 trp1 Δ1 leu2-Δ1 CFVII/RAD2.d.YPH277) URA3 SUP11 chl1-112*	Spencer *et al.*, 1990
YCTF113	*MATa ura3-52 lys2-801 ade2-101 trp1Δ1 leu2-Δ1 CFVII(RAD2.d.YPH277) URA3 SUP11 chl1-113*	Spencer *et al.*, 1990
YPH275	*MATa/MATα ura3-52/ura3-52 lys2-801/lys2-801 ade2-101/ade2-101 his3-Δ200/his3-Δ200 trp1-Δ1/trp1-Δ1 leu2Δ1/leu2Δ1 CFVII(RAD2.d.YPH275)TRP1SUP11*	
YPH279	*MATa/Matα ura3-52/ura3-52 lys2-801/lys2-801 ade2-101/ade2-101 HIS3/his3-*Δ200 TRP1/trp1-*Δ1 leu2Δ1/leu2-Δ1 CFVII(RAD2.d.YPH277)URA3 SUP11*	
YPH576	*MATa ura3 ade2-101 leu2 chl1-1 CFVII(RAD2.d.YPH277)URA3 SUP11*	Spencer *et al.*, 1990
YPH695	*MATa ura3-52 lys2-801 ade2-101 his3-Δ200 trp1-Δ1*	
YPH696	*MATα ura3-52 lys2-801 ade2-101 his3-Δ200 trp1-Δ1 leu2-Δ1*	
YPH697	*MATa ura3-52 lys2-801 ade2-101 his3-Δ200 trp1-Δ1 ctf1Δ1::HIS3*	YPH695, *chl1Δ1::HIS3*
YPH698	*MATα ura3-52 lys2-801 ade2-101 his3-Δ200 trp1-Δ1 leu2-Δ1 cft1Δ1::HIS3*	YPH696, *chl1Δ1::HIS3*
YPH699	*MATa/MATα ura3-52/ura3-52 lys2-801/lys2-801 ade2-101/ade2-101 his3-Δ200/his3-Δ200 trp1-Δ1/trp1Δ1 LEU2/leu2-Δ1*	YPH695/YPH696
YPH700	*MATa/MATα ura3-52/ura3-52 lys2-801/lys2-801 ade2-101/ade2-101 his3-Δ200/his3-Δ200 trp1-Δ1/trp1Δ1 LEU2/leu2-Δ1 ctf1Δ1::HIS3 ctf1Δ1::HIS3*	YPH697/YPH698
YPH702	*MATa/MATα ura3-52/ura3-52 lys2-801/lys2-801 ade2-101/ade2-101 his3-Δ200/his3-Δ200 trp1-Δ1/TRP1 leu2-Δ1/leu2-Δ1 CTF1::In43His3/ctf1-32*	This study
YPH715	*MATa/MATα ura3-52/ura3-52 lys2-801/lys2-801 ade2-101/ade2-101 his3-Δ200/his3-Δ200 trp1-Δ1/trp1Δ1 leu2-Δ1/leu2-Δ1 CHL1/chl1::In19HIS3.*	YPH275 transformed *with In19*
YPH716	*MATa/MATα ura3-52/ura3-52 lys2-801/lys2-801 ade2-101/ade2-101 his3-Δ200/his3-Δ200 trp1-Δ1/trp1Δ1 leu2-Δ1/leu2-Δ1 CHL1/chl1::In47HIS3*	YPH275 transformed *with In47*
YPH717	*MATa ura3-52 lys2-801 ade2-101 his3-Δ200 trp1-Δ1 leu2-Δ1 chl1::In19HIS3*	Meiotic product of YPH715
YPH718	*MATa ura3-52 lys2-801 ade2-101 his3-Δ200 trp1-Δ1 leu2-Δ1 chl1::In47HIS3*	Meiotic product of YPH716
YPH719	*MATa/MATα ura3-52/ura3-52 lys2-801/lys2-801 ade2-101/ade2-101 his3-Δ200/his3-Δ200 trp1-Δ1/trp1Δ1* leu2-*Δ1/leu2-Δ1 chl1::In19/chl1::In19HIS3*	Zygote from meiotic products of YPH715
YPH720	*MATa/MATα ura3-52/ura3-52 lys2-801/lys2-801 ade2-101/ade2-101 his3-Δ200/his3-Δ200 trp1-Δ1/trp1Δ1* leu2-*Δ1/leu2-Δ1 chl1::In47HIS3/chl1::Tn47HIS3*	Zygote from meiotic product of YPH716
7885-1a	*MATa ura3-52 lys2-801 ade2-101 his3-Δ200 trp1-Δ1 leu2-Δ1 rad9::His3*	T.Weinert (YPH736)
7885-3c	*MATα ura3-52 lys2-801 ade2-101 his3-Δ200 trp1-Δ1 leu2-Δ1 rad9::His3*	T.Weinert (YPH738)
7885-2b	*MATα ura3-52 lys2-801 ade2-101 his3-Δ200 trp1-Δ1 leu2-Δ1*	T.Weinert (YPH737)
7885-4d	*MATa ura3-52 lys2-801 ade2-101 his3-Δ200 trp1-Δ1 leu2-Δ1*	T.Weinert (YPH739)
YPH743	*MATa ura3-52 lys2-801 ade2-101 his3-Δ200 trp1-Δ1 leu2-Δ1 rad9::HIS3 chl1Δ1::TRP1*	7885-1a *chl1Δ1::TRP1*
YPH744	*MATα ura3-52 lys2-801 ade2-101 his3-Δ200 trp1-Δ1 leu2-Δ1 chl1Δ1TRP1*	7885-2b *chl1Δ1::TRP1*
YPH745	*MATa/MATα ura3-52/ura3-52 lys2-801/lys2-801 ade2-101/ade2-101 his3-Δ200/his3-Δ200 trp1-Δ1/trp1Δ1* leu2-*Δ1/leu2-Δ1 CHL1/chl1::In43HIS3*	YPH275 transformed with In43

Continued...
Table IV. Strains used in this study[a]

S.cerevisiae strain S288C derivatives	Genotype	Source or reference
YPH746	*MATa ura3-52 lys2-801 ade2-101 his3-Δ200 trp1-Δ1 leu2-Δ1 chl1::In43HIS3*	Meiotic product of YPH745
YPH747	*MATa/MATα ura3-52/ura3-52 lys2-801/lys2-801 ade2-101/ade2-101 his3-Δ200/his3-Δ200 trp1-Δ1/trp1Δ1* leu2-*Δ1/leu2-Δ1 chl1Δ1::TRP1/chl1Δ1::TRP1*	Zygote from YPH744/ YPH754
YPH748	*MATa/MATα ura3-52/ura3-52 lys2-801/lys2-801 ade2-101/ade2-101 his3-Δ200/his3-Δ200 trp1-Δ1/trp1Δ1* leu2-*Δ1/leu2-Δ1 rad9::His3/rad9::HIS3*	Zygote from 7885-1a/ 7885-3c
YPH749	*MATa/MATα ura3-52/ura3-52 lys2-801/lys2-801 ade2-101/ade2-101 his3-Δ200/his3-Δ200 trp1-Δ1/trp1Δ1* leu2-*Δ1/leu2-Δ1*	Zygote from 7885-2b/ 7885-4d
YPH750	*MATa/MATα ura3-52/ura3-52 lys2-801/lys2-801 ade2-101/ade2-101 his3-Δ200/his3-Δ200 trp1-Δ1/trp1Δ1* leu2-*Δ1/leu2-Δ1 rad9::HIS3/rad9::HIS3 chl1Δ1::TRP1/chl1Δ1::TRP1*	Zygote from YPH743/ YPH751
YPH751	*MATα ura3-52 lys2-801 ade2-101 his3-Δ200 trp1-Δ1 leu2-Δ1 rad9::HIS3 chl1Δ1::TRP1*	7885-3c *chl1Δ1::TRP1*
YPH754	*MATa ura3-52 lys2-801 ade2-101 his3-Δ200 trp1-Δ1 leu2-Δ1 chl1Δ1TRP1*	7885-4d *chl1Δ1::TRP1*
YPH770	*MATa/MATα ura3-52/ura3-52 lys2-801/lys2-801 ade2-101/ade2-101 HIS3/his3-Δ200 TRP1/trp1Δ1 leu2Δ1/leu2-Δ1 chl1-71/chl1-157 CFVII(RAD2.d.YPH275)URA3 SUP11*	This study
YPH771	*MATa/MATα ura3-52/ura3-52 lys2-801/lys2-801 ade2-101/ade2-101 HIS3/his3-Δ200 TRP1/trp1Δ1 leu2Δ1/leu2-Δ1 chl1-37/chl1-112 CFVII(RAD2.d.YPH275)URA3 SUP11*	This study
YPH772	*MATa/MATα ura3-52/ura3-52 lys2-801/lys2-801 ade2-101/ade2-101 HIS3/his3-Δ200 TRP1/trp1Δ1 leu2Δ1/leu2-Δ1 chl1-68/chl1-157 CFVII(RAD2.d.YPH275)URA3 SUP11*	This study
S.cerevisiase strain: A364a derivatives		
JB281 *MATa ade1-100 ura3-52 his4-519 leu2-3,112*		J.Boeke (YPH725)

[a]Fragment nomenclature; Gerring *et al.*, 1990; Spencer *et al.*, 1990. *CFVII*(RAD2.d.YPH277): a chromosome fragment derived from the *RAD2* distal portion of chromosome VII. *CFIII* (CENIII.L. YPH278): a chromosome fragment derived from the left arm of chromosome III.
[b]The original *ctf* mutant isolates were given consecutive numbers and the corresponding strains designated YCTF1-n. Allele numbers within complementation groups correspond to these original isolate numbers. *ctf1* alleles have been redesignated *chl1*.

delay in *chl1* mutants could be due to a role for *CHL1* itself in the regulation of cell cycle progression in G_2/M. In this case, the chromosome loss phenotype would be the consequence of a delay during this period of the cell cycle.

If *CHL1* has a role in the physical execution of processes directly involved in chromosome transmission, then the G_2/M delay may be the consequence of a checkpoint control mechanism. During G_2/M, a feedback control may be activated in response to the detection of errors caused by the absence of *CHL1*. One well-documented control point, requiring *RAD9*, can induce a transient G_2/M delay in response to X-ray or UV irradiation induced DNA damage (Weinert and Hartwell, 1988). We have shown the *chl1* G_2/M delay to be independent of *RAD9*. This suggests that *chl1* does not incur DNA damage of the type, or at the time in the cell cycle, that is normally surveyed by *RAD9*. This does not rule out the existence of other control mechanisms that may be imposing a G_2/M delay in *chl1* null populations. There are several observations in the literature that suggest the existence of other control mechanisms acting in *S.cerevisiae* at this stage of the cell cycle. An accumulation of cells with a G_2/M content of DNA is observed for mutants containing dominant alleles of *CLN3*, which encodes a G_1 cyclin (*DAF1-1*, Cross, 1988; *WHI-1*, Nash *et al.*, 1988). Phenotypes consistent with a G_2/M cell cycle delay are also seen in response to multiple circular CEN/ARS plasmids (Futcher and Carbon, 1986), dicentric plasmids (Koshland *et al.*, 1987), and cells with 10 kb short linear chromosomes (A.Murray, personal communication).

The absence of *chl1* might cause a physical barrier to a process involved in chromosome transmission leading to a G_2/M delay that is eventually overcome, with consequent chromosome missegregation. This issue can be addressed once we better understand the biochemical properties of *CHL1* (see below).

A direct role for *CHL1* in regulating progression through the cell cycle requires that a G_2/M delay lead to dramatic chromosome loss. Conceivably, arrest of the cell cycle at a stage in which chromosomes are metastable might lead to unscheduled chromosome structural changes, and subsequent chromosome loss. However, delays of comparable magnitude induced with 2 krad X-irradiation (T.Weinert, personal communication) or with 10 μg/ml Benomyl (R.Li and A.Murray, personal communication),

and an M arrest induced with 100 μM nocadzole (D.Koshland, personal communication), cause essentially no decrease in the mitotic stability of chromosomes. In addition, the *DAF1-1* mutation, which leads to a G_2/M accumulation of cells, does not exhibit a significant increase in chromosome loss (F.Cross, personal communication). It is possible that the *chl1* G_2/M delay may differ in property from the delays induced by these means. Nevertheless, this model for *CHL1* function seems unlikely.

From the comparison of *CHL1* and *RAD3* deduced proteins, four domains exhibiting a high percentage of identical residues were defined. Three of these regions show homology to consensus sequences associated with known biochemical activities. Two domains (I and II) correspond to an ATP binding site consensus (Walker *et al.*, 1982), with some resemblance to a recently defined helicase consensus sequence (Linder *et al.*, 1989). *RAD3* protein has been shown to have ATPase and helicase activities *in vitro* (Sung *et al.*, 1987a,b; Harosh *et al.*, 1989). Both activities are abolished by a lysine to arginine mutation in the A box of this ATP binding site consensus (Sung *et al.*, 1988). The corresponding region also appears to be important for *CHL1* function. Mutant *chl1* alleles that substitute conservative amino acid changes for K48 or G47 within the A box are unable to complement the chromosome loss phenotype of a *chl1* deletion strain (S.L.Gerring and P.Hieter unpublished).

Another region of high identity between the two proteins (Domain IV, Figure 6) has properties suggesting the formation of a helix-turn-helix structure (Naumovski *et al.*, 1985) found in many DNA binding proteins (reviewed in Pabo and Sauer, 1984). Inspection of this region reveals that the three most important helix-turn-helix motif residues (A, G and I at the appropriate spacing) are conserved, but that the pattern of hydrophilic and hydrophobic residues around the conserved glycine and at the beginning of the second helix are unusual for a helix-turn-helix. The potential for helix-turn-helix structure in this region is therefore unclear. A role for this region in DNA binding has not yet been tested for either *CHL1* or *RAD3*.

The overall percentage identity between the two proteins is low (23%) and the degree of functional similarity between the *CHL1* and *RAD3* proteins is unknown. Of relevance to this observation, radiation sensitivity, a characteristic of *RAD3* mutants (Nauvmoski and Friedberg, 1986) is not a phenotypic property of *chl1* mutants (Liras *et al.*, 1978; Spencer *et al.*, 1990). In addition, overexpression of *RAD3* does not complement the *chl1* chromosome fragment loss defect (S.L.Gerring and P.Hieter unpublished). It is possible therefore, that the overall relatedness of the two proteins is simply a reflection of the structural constraints imposed on two proteins that perform similar enzymatic functions in different pathways.

We have identified two PEST sequences (Rogers *et al.*, 1986) as evidenced by high PEST sequence scores within the *CHL1* predicted protein. PEST sequences of this 'strength' have only been found in proteins with short half-lives, suggesting that *CHL1* is an unstable protein. The significance of these sequences for *CHL1* function and stability, and their relevance to the levels of *CHL1* protein present at different stages of the cell cycle are currently being tested.

Our results suggest that *CHL1* is an ATP binding protein that functions after DNA synthesis and before the completion of mitosis (2:0 missegregation, high rates of chromosome III loss, near wild-type rates of recombination, and a G_2/M delay that is *RAD9* independent). We speculate that *CHL1* is an ATPase that may interact with chromosomal DNA and whose absence, revealed in G_2/M, leads to sister chromatid missegregation. Further analysis will clarify the precise role of *CHL1* in chromosome transmission and its potential interactions with checkpoint control mechanisms operating within G_2/M.

Materials and methods

Yeast strains and media

The yeast strains used in these studies are listed in Table IV. All *ctf1* (*chl1*) mutant strains are derived from a congenic series of strains previously described (Sikorski and Hieter, 1989; Spencer *et al.*, 1990). The *chl1Δ1::HIS3* mutation was constructed *in vitro* and used to replace the wild-type locus via an alternate one step gene replacement technique, 'γ replacement' (Sikorski and Hieter, 1989). A 0.8 kb *Eco*RI–*Spe*I fragment directly upstream of *CHL1* and an internal 1 kb *Xba*I–*Eco*RI sequence were cloned in a tandem but reversed order into a *HIS3*-based integrating vector, pRS303 (Sikorski and Hieter, 1989) to form pγ16RI. This construct was linearized with *Eco*RI and used to replace 1.7 kb of the *CHL1* ORF (between the *Spe*I and *Xba*I sites which includes the first AUG, Figure 6) with pRS303 vector sequences via 'γ replacement'. This construct deletes the amino terminal half of the *CHL1* predicted protein. *chl1Δ1::TRP1* is similar to *chlΔ1::HIS3* except pRS304 replaces pRS303. Insertional mutagenesis of *CHL1* cloned DNA with Tn*3*::*HIS3* transposons was carried out in *E.coli* as described (Seifert *et al.*, 1986). A yeast centromere plasmid, pSL40, described below, containing a 6.0 kb insert of the *CHL1* complementing clone flanked by vector-derived *Not*I sites (pS35, Figure 3) was used as the transposon target. 6/96 independent transposon insertions were within the insert as evidenced by *Not*I restriction mapping. The corresponding yeast genomic insertion mutations were made by one-step gene replacement using these *Not*I restriction fragments [named by insertion number (In) as shown in Figure 3] and selecting His^+ yeast transformants. Media for yeast growth and sporulation were as described (Sherman *et al.*, 1986) except that adenine was added at 6 μg/ml to minimal (SD) media to enhance red pigment formation in *ade2* backgrounds (Hieter *et al.*, 1985).

Analysis of chromosome III missegregation and MATαhomozygosis rates

Quantitative measurement of chromosome III loss and recombination was performed by fluctuation analysis essentially as previously described (Spencer *et al.*, 1990). Strains to be tested were plated to single cells on YPD plates and allowed to grow at 30°C to colonies consisting of ~50 000 cells. Ten colonies were plugged from the agar with a sterile Pasteur pipet for each experiment and resuspended in 100 μl YPD. 0.05% of these cells were plated on YPD to determine viable cell numbers. Mating was initiated by adding the remaining cells to 500 000 *MATa* haploid testers (YPH725) in a final volume of 145 μl. After 6 h at 30°C the mating mixture was plated on medium selecting for prototrophic triploids. The colonies that formed were counted and scored for a Leu^+ phenotype by replica plating to minimal medium lacking leucine. Wild-type *MATα* haploids were used as a control to determine mating efficiency. The number of maters obtained in each experiment was corrected based on this efficiency. To ensure that the rate of *MATα* homozygosis or chromosome III missegregation was not underestimated due to a mating defect associated with *chl1*, a control *chl1* null haploid YPH698, was tested. This revealed no significant mating deficiency associated with *chl1Δ1::HIS3*. The combined rate of *MATα* homozygosis plus chromosome III loss was determined from the total number of cells that mated by the method of the median (Lea and Coulson, 1948). The rate of chromosome III loss was calculated by subtracting the rate of mitotic recombination between CENIII and *MATα* [determined by P_0 analysis of Leu^+ maters (Luria and Delbruck, 1943)] from the combined rate. Results varied by no more than a factor of two upon experimental repeat.

Cloning CHL1

CHL1 was cloned from a library (F.Spencer and P.Hieter, unpublished) of 10–12 kb fragments of yeast genomic DNA inserted into a pBR322-based *LEU2/CEN4/ARS1* shuttle vector pSB32 (J.Trueheart, unpublished). Putative *CHL1*-containing clones were identified by screening Leu^+ transformants for complementation of the sectoring phenotype. These occurred at a

frequency of 1 in 250 YCTF112 transformants and 1 in 1000 YCTF113 transformants. Plasmids were rescued in *E.coli* by transformation of yeast genomic DNA preparations as described previously (Davis *et al.*, 1980). To sublocalize the gene within the cloned DNA segments, the smallest of the three genomic clones obtained, pCTF1-C, was partially digested with *Sau*3A, and 2–4 kb fractions were agarose gel purified and shotgun cloned into the *Bam*HI site of a kanamycin-based *CEN4/LEU2/ARS1* shuttle vector pSL40 (S.Lee and P.Hieter, unpublished). pSL40 was constructed by inserting a 5 kb *LEU2/CEN4/ARS1* fragment into the *Sma*I site of pHSS6 (Seifert *et al.*, 1986). *chl1* complementing subclones were identified by their ability to complement the sectoring phenotype of *chl1* mutants. Transposition mutagenesis on the smallest of these pSL40-based *CHL1* subclones (pS35) was performed as described (Seifert *et al.*, 1986) using the *HIS3*-based Tn*3* transposon. pSR35R and pS35H were constructed by cloning the appropriate *Eco*RI and *Hin*dIII fragments, respectively (Figure 3), into a *HIS3/CEN6/ARSH4* based vector, pRS313 (Sikorski and Hieter, 1989). Proof that the cloned DNA corresponded to the *CHL1* locus was obtained as follows. Haploid strains containing the Tn*3*::*HIS3* transposon insertion In43 (Figure 3) integrated at the genomic site of the cloned DNA, were obtained from the meiotic products of YPH745 (Table IV). These strains exhibited a wild-type sectoring phenotype since In43 does not perturb *CHL1* function (Figure 3). A diploid YPH702 was constructed by mating this strain with a *his3 chl1-32* haploid (Table IV). YPH702 was sporulated and tetrads dissected. Of the 42 chromosome fragment-containing spores in 21 four-spored-tetrads, all were either His^- Chl^- or His^+ Chl^+.

Chromosome assignment and physical map position of CHL1

The mapping methods used were as previously described (Vollrath *et al.*, 1988. Gerring *et al.*, 1990). To map the position of *CHL1* on chromosome XVI, a 3.5 kb *CHL1*-containing *Eco*RI fragment (Figure 3) was cloned in both orientations into the chromosome fragmentation vectors YCF3 and YCF4 (Vollrath *et al.*, 1988). These constructs were linearized to reveal free ends in the *CHL1* sequences and the telomere adjacent Y′ sequences and used to transform yeast strain YPH49 by the lithium acetate procedure (Ito *et al.*, 1983). Depending on the orientation of *CHL1* in the vectors, stably maintained 'chromosome fragments' are generated with either all sequences proximal to *CHL1* (acentric vector) or with all sequences distal to *CHL1* (centric vector). The sizes of these chromosome fragments were determined by OFAGE analysis (Carle and Olson, 1984). The *GAL4* probe used was a 3 kb *Bam*HI–*Eco*RI fragment of pS46-1, obtained from P.Silver via J.Boeke. Probes were radioactively labeled with ^{32}P using the Feinberg method (Feinberg and Vogelstein, 1983).

Sequence analysis

Subclones of *CHL1* were obtained for sequence analysis essentially as described (Henikoff, 1987) by performing exonuclease III deletions from both directions on the *Eco*RI genomic insert of pS35R cloned into the phagemid vector *HIS3/CEN6/ARSH4* vector pRS313 (Sikorski and Hieter, 1989). Single stranded DNA templates were obtained by rescue with helper phage R408 (Stratagene) and sequenced by chain termination reactions (Sanger *et al.*, 1977). The last two amino acids of *CHL1* were truncated at the C-terminal end of this fragment at the *Eco*RI site, but sequence across this junction was obtained using denatured double stranded templates derived from larger clones. The nucleotide sequence illustrated in Figure 5 was obtained for both DNA strands. GenBank version number 62.0 was translated in all reading frames and tested for similarity with *CHL1* predicted protein. PEST sequence analysis was provided by C.Watanabe using the published PEST sequence analysis program (Rogers *et al.*, 1986). The two PEST sequences underlined in Figure 5 scored between +13.0 and +15.0 using this program. Domains I–IV listed in Figure 6 were arbitrarily defined as regions containing 10 amino acid stretches with seven or more identities and three similarities between *CHL1* and *RAD3* predicted proteins.

Immunofluorescence and cellular morphology

Primary antibodies to α-tubulin (4–124) (Schatz *et al.*, 1987) and β-tubulin (6–345) (Bond *et al.*, 1986) were kindly provided by Frank Solomon. Their immunolocalization was detected with fluorescein isothiocyanate-labeled goat anti-rabbit secondary antibody obtained from Cappel labs. Immunofluorescence was performed as described (Kilmartin and Adams, 1984) with some modifications. Cells grown to an OD_{600} = 1.0 were fixed by adding formaldehyde directly to the growth medium to a final concentration of 3.7%, with gentle mixing. After 1 h at room temperature these cells were washed twice in SK buffer (1 M sorbitol, 50 mM potassium phosphate pH 7.5). The cells were concentrated 5-fold after resuspension in SK buffer which was then made 0.05% v/v β-glucuronidase (Boehringer Mannheim GmbH), 5 μg/ml 100T zymolase (ICN), and 0.01% β-mercaptoethanol (Sigma). After a 1 h incubation at 37°C, cells were pelleted and further concentrated 4-fold in the final resuspension in SK buffer. 10 μl of these cells were placed on polylysine coated slides (precoated with a 0.1% polylysine solution, rinsed and air dried), allowed to settle, and the supernatant was aspirated off. To prevent non-specific binding, samples were treated with 20 μl of BSA-PBS (0.1% bovine serum albumin, 150 mM NaCl) 50 mM potassium phosphate, pH 7.5) in a moist chamber for 30 min. This solution was aspirated off and replaced with 10 μl of a mixture of the two anti-tubulin primary antibodies each diluted 1:1000 in BSA-PBS, and incubated 1 h to overnight at 25°C. Slides were rinsed five times with BSA-PBS, and incubated with 10 μl secondary antibody (diluted 1:1000 in BSA-PBS) for 1 h at 25°C in the dark. After three rinses with BSA-PBS, slides were mounted in 90% glycerol, 0.1× PBS, 0.1% *p*-phenylenediamine and 0.01% 4′,6-diamidino-2-phenylindole (DAPI, obtained from Sigma). A Zeiss selective fluorescein isothiocyanate filter was used for viewing microtubules and a Zeiss selective UV filter was used for viewing DAPI stained material. Cell size was determined from cell length (l) and diameter (d) measurements at bud initiation. Cell volume was calculated by assuming an ellipsoid cell shape, and using the volume formula for an ellipse. The average cell volume ratio of *chl1* to *CHL1* determined by coulter channelizer was similar to that obtained by this measurement. Cell viability of unusually large budded cells was determined by microdissection to be 84% (16/19), 88% (21/24), 58% (11/19) and 84% (26/31) respectively for YPH47, YPH697, YPH49 and YPH700. Overall cell viability was assessed by plating a known number of cells (determined by a haemocytometer after brief sonication) on non-selective medium. The viability calculated was 85%, 83%, 100% and 100% respectively for YPH47, YPH697, YPH699 and YPH700.

Flow cytometry

Yeast cells were prepared for flow cytometry using a method modified from Hutter and Eipel (1978). 1 ml of a logarithmically growing culture (OD_{600} = 0.3–0.8) grown in liquid YPD were pelleted and resuspended in 250 mM Tris pH 7.5, sonicated for 10 s, and fixed in 75% (v/v) ethanol for 1 h at room temperature. Cells were pelleted, washed once with SCE buffer (1 M sorbitol, 0.1 M sodium citrate pH 5.8, 10 mM EDTA), and resuspended in 200 μl SCE buffer containing 1 mg/ml pancreatic RNase A (Sigma). After a 1 h incubation at 37°C, cells were pelleted and resuspended in 500 μl fresh pepsin solution [0.05% pepsin (w/v) in 0.55 N HCl]. After a 5 min incubation at room temperature, the cells were washed twice with SCE and resuspended to a final volume of 500 μl. These cells were diluted to an OD_{600} of 0.1 in SCE and brought to 2.9 μg/ml propidium iodide (Sigma). Flow cytometric analysis was performed 1 h later on a Coulterepics 752 apparatus with the gain set at 10 and the high voltage set a 925 V. Propidium iodide stained cells were excited with 300 mW 480 nm light and integrated red (≥590 nm) fluorescence was recorded.

Acknowledgements

We would like to thank Bertha Robinson and Quentin Burley for technical support, Jim Flook for assistance with flow cytometric analysis, Jim Haber for the *Chl1-1* strain, Ted Weinert for *rad9* strains and Louise Prakash for pSCW367. We would also like to thank Andrew Murray, Ted Weinert and Susan Michaelis for critical reading of the manuscript, Mark Rose for helpful discussions, and Mark Goebl, Mark Boguski, Colin Watanabe, Carl Pabo and Lesa Beamer for assistance with sequence analysis. This work was supported by grants from the Public Health Service (CA16519) and the Pew Memorial Trust (86–909GHE) to P.H., a departmental N.I.H. training grant to S.G. (5T32CA09139-15), and a Monsanto fellowship to F.S.

References

Bond,J.F., Fridovich-Keil,J.L., Pillus,L., Mulligan,R. and Solomon,F. (1986) *Cell*, **44**, 461–468.
Carle,G.F. and Olson,M. (1984) *Nucleic Acids Res.*, **12**, 5647–5665.
Cross,F.R. (1988) *Mol. Cell. Biol.*, **8**, 4675–4684.
Dayhoff,M.O., Barker,W.C. and Hunt,L.T. (1983) *Methods Enzymol.*, **91**, 524–545.
Davis,R.W., Thomas,M., Cameron,J., St John,T.P., Scherer,S. and Padgett,P.A. (1980) *Methods Enzymol.*, **65**, 404–411.
Feinberg,A.P. and Vogelstein,B. (1983) *Anal. Biochem.*, **132**, 6–13.
Foury,F. and Lahaye,A. (1987) *EMBO J.*, **6**, 1441–1449.
Friedberg,E.C. (1988) *Microbiol. Rev.*, **52**, 70–102.
Futcher,B. and Carbon,J. (1986) *Mol. Cell. Biol.*, **6**, 2213–2222.
Gerring,S.L., Connelly,C. and Hieter,P.H. (1990) *Methods Enzymol.*, **194**, 57–77.
Haber,J. (1974) *Genetics*, **78**, 843–858.

Harosh,I., Naumovski,L. and Freidberg,E.C. (1989) *J. Biol. Chem.*, **264**, 20532–20539.
Hartwell,L.H. and Smith,D. (1985) *Genetics*, **110**, 381–395.
Hartwell,L.H. and Weinert,T.A. (1989) *Science*, **246**, 629–634.
Henikoff,S. (1987) *Methods Enzymol.*, **155**, 156–165.
Hieter,P., Mann,C., Snyder,M. and Davis,R. (1985) *Cell*, **40**, 381–392.
Hutter,K.J. and Eipel,H.E. (1978) *Antonie Leeuwenhoek J. Microbiol. Serol.*, **44**, 269–282.
Ito,H., Fukuda,Y., Murata,K. and Kimura,A. (1983) *J. Bacteriol.*, **153**, 163–168.
Kilmartin,J.V. and Adams,A.E.M. (1984) *J. Cell. Biol.*, **98**, 922–933.
Koshland,D. and Hieter,P. (1987) *Methods Enzymol.*, **155**, 351–372.
Koshland,D., Rutledge,L., Fitzgerald-Hayes,M. and Hartwell,L. (1987) *Cell*, **48**, 801–812.
Lea,D.E. and Coulson,C.A. (1948) *J. Genet.*, **49**, 264–284.
Linder,P., Lasko,P.F., Ashburner,M., Leroy,P., Nielson,P., Nishi,K., Schnier,J. and Slonimski,P.P. (1989) *Nature*, **337**, 121–122.
Lipman,D.J. and Pearson,W.R. (1985) *Science*, **227**, 1435–1441.
Liras,P., McCusker,J., Mascioli,S. and Haber,J. (1978) *Genetics*, **88**, 651–671.
Luria,S.E. and Delbruck,M. (1943) *Genetics*, **28**, 491.
Nash,R., Tokiwa,G., Anand,S., Erickson,K. and Futcher,A.B. (1988) *EMBO J.*, **7**, 4335–4346.
Naumovksi,L. and Friedberg,E.C. (1986) *Mol. Cell. Biol.*, **6**, 1218–1227.
Naumovski,L., Chu,G., Berg,P. and Friedberg,E.C. (1985) *Mol. Cell. Biol.*, **5**, 17–26.
Newlon,C. (1988) *Microbiol. Rev.*, **52**, 568–601.
Pabo,C.O. and Sauer,R.T. (1984) *Annu. Rev. Biochem.*, **53**, 293–321.
Reed,S. (1980) *Genetics*, **95**, 561–577.
Reynolds,P., Higgins,D.R., Prakash,L. and Prakash,S. (1985) *Nucleic Acids Res.*, **13**, 2357–2372.
Rogers,S., Wells,R.and Reichsteiner,M. (1986) *Science*, **234**, 364–369.
Russel,P., Moreno,S. and Reed,S.I. (1989) *Cell*, **57**, 295–303.
Sanger,F., Nicklen,S. and Coulson,A.R. (1977) *Proc. Natl. Acad. Sci. USA*, **74**, 5463–5467.
Schatz,P.J., Georges,G.E., Solomon,F. and Botstein,D. (1987) *Mol. Cell. Biol.*, **7**, 3799–3805.
Schiestl,R.H., Reynolds,P., Prakash,S. and Prakash,L. (1989) *Mol. Cell. Biol.*, **9**, 1882–896.
Seifert,H.S., Chen,E.Y., So,M. and Heffron,F. (1986) *Proc. Natl. Acad. Sci. USA*, **83**, 735–739.
Sherman,F., Fink,G.R. and Hicks,J.B. (1986) *Methods in Yeast Genetics: Course Manual*. Cold Spring Harbor Laboratory Press, Cold Spring Harbor, NY.
Sikorski,R.S. and Hieter,P. (1989) *Genetics*, **122**, 19–27.
Spencer,F., Gerring,S.L., Connelly,C. and Hieter,P. (1990) *Genetics*, **124**, 237–239.
Sung,P., Prakash,L., Matson,S.W. and Prakash,S. (1987a) *Proc. Natl. Acad. Sci. USA*, **84**, 8951–8955.
Sung,P., Prakash,L., Weber,S. and Prakash,S. (1987b) *Proc. Natl. Acad. Sci. USA*, **84**, 6045–6049.
Sung,P., Higgins,D., Prakash,L. and Prakash,S. (1988) *EMBO J.*, **7**, 3263–3269.
Vollrath,D., Davis,R., Connelly,C. and Hieter,P. (1988) *Proc. Natl. Acad. Sci. USA*, **85**, 6027–6031.
Walker,J.E., Saraste,M., Runswick,M.J. and Gay,N.J. (1982) *EMBO J.*, **1**, 945–951.
Weinert,T.A. and Hartwell,L. (1988) *Science*, **241**, 317–322.

Received on August 6, 1990; revised on October 2, 1990

Note added in proof

The *CHL1* sequence has been given the accession number X56584.